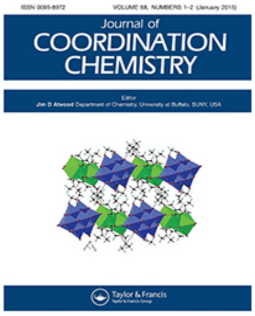

Taylor & Francis
Taylor & Francis Group

Journal of Coordination Chemistry

ISSN: 0095-8972 (Print) 1029-0389 (Online) Journal homepage: http://www.tandfonline.com/loi/gcoo20

Synthesis, structures and luminescent properties of two zinc(II) complexes from flexible bis(tetrazolate) ligands

Xiaoju Li, Zhifa Li, Xiahong Xu & Xiaofang Guo

To cite this article: Xiaoju Li, Zhifa Li, Xiahong Xu & Xiaofang Guo (2015) Synthesis, structures and luminescent properties of two zinc(II) complexes from flexible bis(tetrazolate) ligands, Journal of Coordination Chemistry, 68:2, 195-205, DOI: 10.1080/00958972.2014.983914

To link to this article: http://dx.doi.org/10.1080/00958972.2014.983914

Journal of Coordination Chemistry, 2015
Vol. 68, No. 2, 195–205, http://dx.doi.org/10.1080/00958972.2014.983914

Synthesis, structures and luminescent properties of two zinc (II) complexes from flexible bis(tetrazolate) ligands

XIAOJU LI*†‡, ZHIFA LI†‡, XIAHONG XU†‡ and XIAOFANG GUO†‡

†Fujian Key Laboratory of Polymer Materials, College of Chemistry and Chemical Engineering, Fujian Normal University, Fuzhou, China
‡College of Materials Science and Engineering, Fujian Normal University, Fuzhou, China

(*Received 14 October 2013; accepted 16 August 2014*)

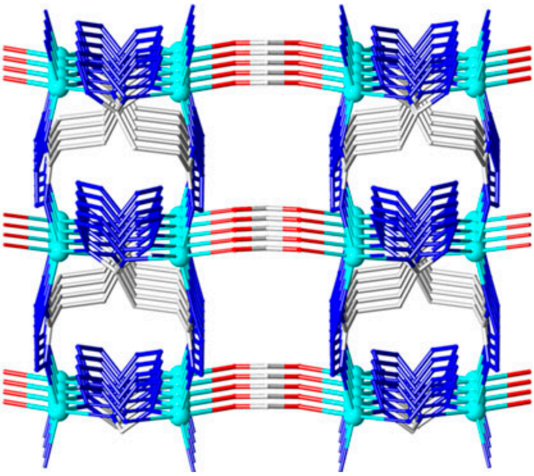

Two unprecedented Zn(II) coordination polymers based on flexible 1,2-di(1H-tetrazol-5-yl)ethane (H_2dte) and 1H-tetrazol-5-yl)propane (H_2dtp) have been prepared. The dte^{2-} and dtp^{2-} ligands link three Zn(II) ions into a 2-D layer and a 1-D chain, respectively. These are further extended into 3-D and 2-D networks by *in situ* formed formate and hydroxyl bridges.

Two Zn(II) coordination polymers, $[Zn_2H(dte)_2(HCOO)\cdot(H_2O)\cdot(CH_3OH)]_n$ (**1**) and $[Zn_2(dtp)(OH)_2]_n$ (**2**), with flexible 1,2-di(1H-tetrazol-5-yl)ethane (H_2dte) and 1,2-di(1H-tetrazol-5-yl)propane (H_2dtp) have been prepared. The dte^{2-} and dtp^{2-} ligands adopt chelating and bridging coordination, and link three Zn(II) ions into a 2-D layer and a 1-D chain, respectively. The anionic formate and hydroxyl bridges are formed *in situ*, which further extend the 2-D layer and the 1-D chain into 3-D and 2-D networks, respectively. Complexes **1** and **2** showed a maximum fluorescent emission at 403 and 422 nm, respectively.

Keywords: Coordination polymer; Crystal structure; Zinc(II); Fluorescence; Tetrazolate

---

*Corresponding author. Email: xiaojuli@fjnu.edu.cn

1. Introduction

There is a significant interest in the development of materials with high energy densities, owing to their promising application as aerospace propellants and explosives [1]. Much effort has been focused on the design and synthesis of five-membered, nitrogen-rich, energetic heterocyclic compounds [2–4]. In this context, tetrazole is a promising energetic precursor owing to its high nitrogen content, high positive heat of formation, and good thermal stability [4]. Tetrazole derivatives are readily available in high yields through simple cycloaddition reactions between organic azides and cyano compounds. The assembly of tetrazoles with metal cations generates many metal–organic coordination polymers with interesting structures and properties [6–11]. Some have been used as potential primary explosives, gas generators, and additives of low-smoke propellant ingredients in solid rockets [7].

It is well known that the acidity of tetrazole is close to that of a carboxylic acid [12]. Similar to carboxylate ligands, tetrazolate derivatives also possess versatile coordination modes and strong coordination abilities to metal cations [9–15]. A tetrazole may potentially coordinate to four metal cations by its nitrogen atoms although it usually functions as a mono- or bidentate ligand in most of the reported coordination polymers. The assembly of tetrazolate ligands and metal cations is influenced by lot of factors, such as structure of the organic ligands, coordination geometry of the metal cations, type of counter anions, reaction temperature, reaction solvents, and pH of the solution. The judicious selection of tetrazolate ligands bearing different substituents or spacers is especially crucial to the construction of the final frameworks [13–17]. With the development of supramolecular chemistry and crystal engineering, a variety of interesting tetrazolate-based coordination polymers has been investigated. For example, several groups have studied the self-assembly of metal cations and single tetrazolates via *in situ* ligand synthesis and isolated a series of coordination polymers with intriguing structures and luminescent properties [14–17]. Recently, bi- [18] and polytetrazolate ligands [19] have also been employed for the construction of porous frameworks with absorption properties, but tetrazolate ligands with flexible alkyl spacers remain largely unexplored [20, 21]. In comparison with rigid tetrazolate ligands, the different flexibilities and conformations of these alkyl-linked tetrazolate ligands may induce unexpected frameworks with beautiful esthetics and useful properties.

In our previous study, we mainly focused on the design and synthesis of coordination polymers from flexible bis(imidazolyl) ligands [22–25]. Encouraged by the superior energetic performances of metal-tetrazolate complexes over tetrazolate ligands [3–7], we became interested in energetic coordination polymers. The understanding of the assembly processes and coordination modes of metal cations and tertazolate ligands is the first step to develop metal-containing energetic materials. As a continuation of our study on the coordination polymers from flexible ligands, herein, we report the syntheses, structures, and properties of two Zn(II) coordination polymers made with flexible bis(tetrazolate) ligands,

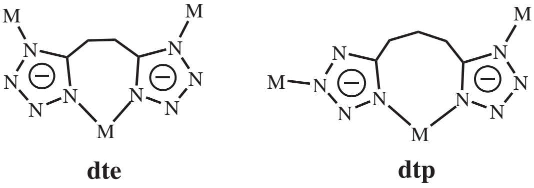

Scheme 1. Coordination modes of dte and dtp.

$[Zn_2H(dte)_2(HCOO)\cdot(H_2O)\cdot(CH_3OH)]_n$ (**1**) and $[Zn_2(dtp)(OH)_2]_n$ (**2**) (H_2dte = 1,2-di(1H-tetrazol-5-yl)ethane, $H_2dt\textit{p}$ = 1,2-di(1H-tetrazol-5-yl)propane) (scheme 1).

2. Experimental

2.1. *Materials and physical measurements*

H_2dte and H_2dtp were synthesized according to the literature methods [26]. Other chemicals were obtained from commercial sources and used without further purification. IR spectra (KBr pellets) were recorded on a Magna 750 FT-IR spectrophotometer from 400 to 4000 cm^{-1}. Fluorescence spectra were obtained on an FLS920 Edinburgh Analytical instrument. Powder X-ray diffraction data were recorded on a PANaytical X'pert pro X-ray diffractometer with graphite-monochromated Cu-Kα radiation (λ = 1.542 Å). Thermogravimetric analysis was carried out on a NETSCHZ STA 449C thermoanalyzer under N_2 at a heating rate of 10 °C min^{-1}. C, H, N elemental analyses were determined on an EA1110 CHNS-0 CE element analyzer.

2.2. *Synthesis of $[Zn_2H(dte)_2(HCOO)\cdot(H_2O)\cdot(CH_3OH)]_n$ (1)*

A mixture of H_2dte (0.20 mM, 33.2 mg), $Zn(NO_3)_2\cdot6H_2O$ (0.60 mM, 178.0 mg), H_2O (15 mL), and MeOH (1.0 mL) was placed in a Teflon-lined stainless steel vessel (30 mL) and was heated to 150 °C for 3 days. After cooling to room temperature at a rate of 10 °C h^{-1}, colorless crystals of **1** (29 mg, 52% yield based on H_2dte) were obtained. The crystals were collected by filtration, washed with H_2O, and dried in air. Anal. Calcd for $C_{10}H_{16}N_{16}O_4Zn_2$ (555.16): C, 21.63; H, 2.90; N, 40.37. Found: C, 21.67; H, 3.25; N, 40.61. IR (KBr, cm^{-1}): 3748(vw), 3443(s), 3378(s), 3043(w), 2503(vw), 2465(vw), 1628 (vs), 1485(s), 1417(s), 1336(s), 1231(m), 1091(m), 1024(w), 890(vw), 801(m), 670(w), 509(w).

2.3. *Synthesis of $[Zn_2(dtp)(OH)_2]_n$ (2)*

A mixture of H_2dtp (0.20 mM, 33.2 mg), $Zn(NO_3)_2\cdot6H_2O$ (0.10 mM, 30.0 mg), $NaN(CN)_2$ (0.20 mM, 18.0 mg), H_2O (15 mL), and MeOH (1.0 mL) was placed in a Teflon-lined stainless steel vessel (30 mL) and was heated to 170 °C for 3 days. After cooling to room temperature at a rate of 10 °C h^{-1}, colorless crystals of **2** (14 mg, 82% yield based on Zn $(NO_3)_2\cdot6H_2O$) were obtained. The crystals were collected by filtration, washed with H_2O, and dried in air. Anal. Calcd for $C_5H_8N_8O_2Zn_2$ (342.99): C, 17.51; H, 2.35; N, 32.67. Found: C, 17.69; H, 2.68; N, 32.75. IR (KBr, cm^{-1}): 3852(vw), 3741(vw), 3524(vs), 2984 (vw), 2930(m), 2374(vw), 1638(m), 1490(s), 1435(vs), 1410(s), 1352(s), 1265(w), 1091 (m), 997(s), 941(s), 648(m), 513(vs).

2.4. *X-ray crystal structural determination*

The single crystals of **1** and **2** were mounted on a glass fiber for X-ray diffraction analysis. Data-sets were collected on a Rigaku Saturn 70 equipped with graphite-monochromated Mo-Kα radiation (λ = 0.71073 Å) from a rotating anode generator at 293 K. Intensities were corrected for LP factors and absorption using the empirical ψ scan technique. The structures were solved by direct methods and refined on F^2 with full-matrix least-squares techniques using the Siemens *SHELXTL* version 5 package of crystallographic software [27]. All non-hydrogen atoms were refined anistropically. The hydrogen atom of the hydroxyl group in **2** was located from the difference Fourier map and refined isotropically. The positions of other hydrogen atoms were generated geometrically (C–H bond fixed at 0.96 Å), assigned

Table 1. Crystal, data collection, and structure refinement parameters for **1** and **2**.

Complex	**1**	**2**
Formula	$C_5H_8N_8O_2Zn$	$C_5H_8N_8O_2Zn_2$
Fw	277.56	342.93
Crystal system	Orthorhombic	Orthorhombic
Space group	$Cmc2_1$	$Pna2_1$
a (Å)	20.071(11)	14.102(13)
b (Å)	9.698(6)	10.140(9)
c (Å)	10.986(6)	6.842(6)
V (Å^3)	2138(2)	978.4(15)
Z	8	4
D_{calcd} (g cm^{-3})	1.724	2.328
μ (mm^{-1})	2.299	4.908
$F(0\ 0\ 0)$	1120	680
Reflections collected	8025	7241
Unique reflections	2442	2078
R_{int}	0.0318	0.0321
GOF	1.073	1.017
$R_1[I > 2\sigma(I)]^a$	0.0309	0.0299
${}_{w}R_2$ (all data)^b	0.0749	0.0574
$\Delta\rho_{\max}$ and $_{\min}$ [e Å^{-3}]	0.839 and −0.305	0.371 and −0.400

$^aR = \sum||F_0|-|F_c||/\sum|F_0|$.
$^b{}_{w}R = [\sum w(F_0{}^2-F_c{}^2)^2/\sum w(F_0{}^2)^2]^{1/2}$.

Table 2. Selected bond lengths (Å) and angles (°) for **1** and **2**.

Complex **1**			
Zn(1)–N(4A)	2.013(3)	Zn(1)–N(5)	2.021(3)
Zn(1)–N(8B)	2.040(3)	Zn(1)–N(1)	2.285(3)
Zn(1)–O(1)	2.149(2)		
N(4A)–Zn(1)–N(5)	112.34(13)	N(4A)–Zn(1)–N(8B)	123.66(13)
N(5)–Zn(1)–N(8B)	123.99(12)	N(4A)–Zn(1)–O(1)	89.30(10)
N(5)–Zn(1)–O(1)	92.42(11)	N(8B)–Zn(1)–O(1)	89.30(10)
N(4A)–Zn(1)–N(1)	97.07(10)	N(5)–Zn(1)–N(1)	88.77(12)
N(8B)–Zn(1)–N(1)	83.94(12)	O(1)–Zn(1)–N(1)	172.53(9)
Complex **2**			
Zn(1)–O(1)	1.924(4)	Zn(1)–O(2)	1.935(4)
Zn(1)–N(1)	2.023(3)	Zn(1)–N(7A)	2.060(3)
Zn(2)–O(2B)	1.928(4)	Zn(2)–O(1C)	1.940(4)
Zn(2)–N(4)	2.038(3)	Zn(2)–N(5)	2.049(3)
O(1)–Zn(1)–O(2)	125.89(11)	O(1)–Zn(1)–N(1)	103.82(16)
O(2)–Zn(1)–N(1)	101.50(17)	O(1)–Zn(1)–N(7A)	107.87(17)
O(2)–Zn(1)–N(7A)	104.00(18)	N(1)–Zn(1)–N(7A)	113.97(12)
O(2B)–Zn(2)–O(1C)	123.46(11)	O(2B)–Zn(2)–N(4)	108.25(18)
O(1C)–Zn(2)–N(4)	103.67(18)	O(2B)–Zn(2)–N(5)	110.93(15)
O(1C)–Zn(2)–N(5)	104.61(15)	N(4)–Zn(2)–N(5)	104.18(12)

Note: Symmetry codes for **1**: (A) $-x + 3/2$, $y - 1/2$, z, (B) x, $-y + 2$, $z + 1/2$; for **2**: (A) x, $y + 1$, z, (B) $-x + 1/2$, $y - 1/2$, $z + 1/2$, (c) $-x + 1/2$, $y - 1/2$, $z - 1/2$.

isotropic thermal parameters, and allowed to ride on their parent carbon atoms before the final cycle of refinement. Crystal, data collection, and structure refinement parameters for **1** and **2** are summarized in table 1. Selected bond distances and angles are given in table 2.

3. Results and discussion

3.1. *Structural description of* $[Zn_2H(dte)_2(HCOO)\cdot(H_2O)\cdot(CH_3OH)]_n$ *(1)*

Single-crystal X-ray diffraction analysis showed that **1** crystallized in the non-centric orthorhombic space group *Cmc2₁*; the Flack parameter is −0.0039 ± 0.0174. As shown in figure 1(a), the Zn(II) atom has a distorted trigonal bipyramidal geometry and is coordinated by four N atoms from three dte^{2-} anions (N1, N5, N4A, and N8B) and one formate O atom O1. Three N atoms from different dte^{2-} ligands (N5, N4A, and N8B) form the equatorial plane with Zn-N bond distances of 2.013(3)–2.039(3) Å, which are similar to those in $[Zn(dtb)(H_2O)_4]_n\cdot(H_2O)_{2n}$ (H_2dtb = 1,2-di(1H-tetrazol-5-yl)butane), where the Zn–N bond distances range from 2.016(14) to 2.046(15) Å [21]. The remaining N atom and formate O atom occupy the axial positions; the O(1)–Zn(1)–N(1) bond angle is 172.53(10)°. The Zn(1)–N(1) and Zn(1)–O(1) bond distances are 2.286(3) and 2.148(2) Å, respectively, which are longer than those in the equatorial plane, suggesting an elongated trigonal bipyramidal geometry. Similar to the dte^{2-} ligand in $[Zn_2(dte)_2(H_2O)]_n$ [21], the dte^{2-} ligand in **1** bridges three Zn(II) atoms in a chelating and bridging coordination mode (scheme 1). The angle between the two tetrazolate rings is 37.753°, and the N2–N3 and N6–N7 bond distances are 1.299(4) and 1.291(4) Å, respectively, which are shorter than the other N–N bond distances (1.364(4)–1.371(4) Å) in the dte^{2-} ligand. The shorter distances are ascribed to the presence of a double bond between the 2- and 3-N atoms in the tetrazolate rings. These N–N bond distances are consistent with the corresponding distances in H_2dte (1.295(2)–1.301(2) and 1.346(2)–1.369(2) Å, respectively), and $[Zn(dte)]_n$ and $[Zn(dte)(H_2O)]_n$ (1.294(4)–1.297(4) and 1.338(3)–1.365(5) Å, respectively) [20]. The two tetrazolate rings of the dte^{2-} ligand adopt a $\mu_{1,4}$-bridging mode to link the adjacent Zn(II) centers into a 2-D layer [figure 1(b)]. The Zn⋯Zn distances across the tetrazolate rings are 6.062 and 6.361 Å. Interestingly, the dte^{2-} ligand links the Zn(II) atoms along a 2_1 screw axis in the direction of crystallographic *c* axis and results in the formation of helical chains with a pitch of 10.104 Å. This helical arrangement can probably be attributed to the steric orientation of tetrazolate rings caused by the flexible $–CH_2CH_2–$ spacer [10]. As shown in figure 1(c), a formate moiety further links the 2-D layers into a 3-D network with 1-D channels. The dimensions of the channels are 5.5 × 5.8 Å. The crystalline methanol and water molecules are located in the 1-D channels as guest molecules, and extensive hydrogen bonding between the water and methanol O atoms [O1 W–H1 W⋯O2^{i} 2.400(1) Å, symmetry code: $-x + 3/2$, $-y + 3/2$, $z + 1/2$; O2–H2O⋯O1 2.948(5) Å, symmetry code: $-x + 1$, y, z] and between the water O atom and a tetrazolate N atom [O1 W–H2 W⋯N3 2.998(8) Å] were observed. A lattice water molecule or one of the N atoms of the tetrazolate rings of the dte^{2-} ligand is required to be protonated to achieve overall charge balance. This proton was difficult to locate crystallographically and may reside on any of the N and O atoms.

3.2. *Structural description of* $[Zn_2(dtp)(OH)_2]_n$ *(2)*

Single-crystal X-ray diffraction analysis showed that **2** was crystallized in the orthorhombic space group *Pna2₁*. As shown in figure 2(a), the asymmetric unit consists of two

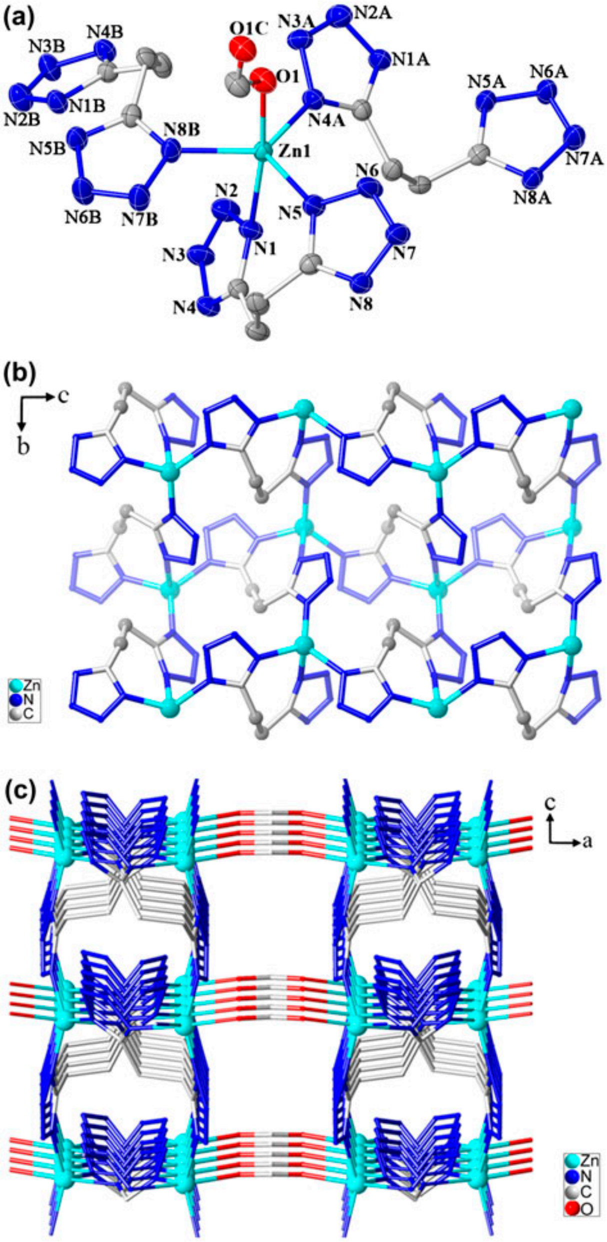

Figure 1. (a) Molecular structure of **1** with 50% thermal ellipsoid probabilities. Hydrogens and crystalline methanol and water molecules were omitted for clarity. Symmetry codes: (A) −*x* + 3/2, *y* − 1/2, *z*, (B) *x*, −*y* + 2, *z* + 1/2; (b) view of 2-D Zn(dte) layer in **1** along the *a* axis; (c) view of the 3-D network in **1** along the *b* axis; crystalline methanol and water molecules were omitted for clarity.

crystallographically independent Zn(II) atoms, one dtp^{2-} anion, and two coordinated hydroxyl groups. Both Zn(1) and Zn(2) have a slightly distorted tetrahedral geometry and are coordinated by two tetrazolate N atoms and two hydroxyl O atoms. Zn(1) is coordinated by

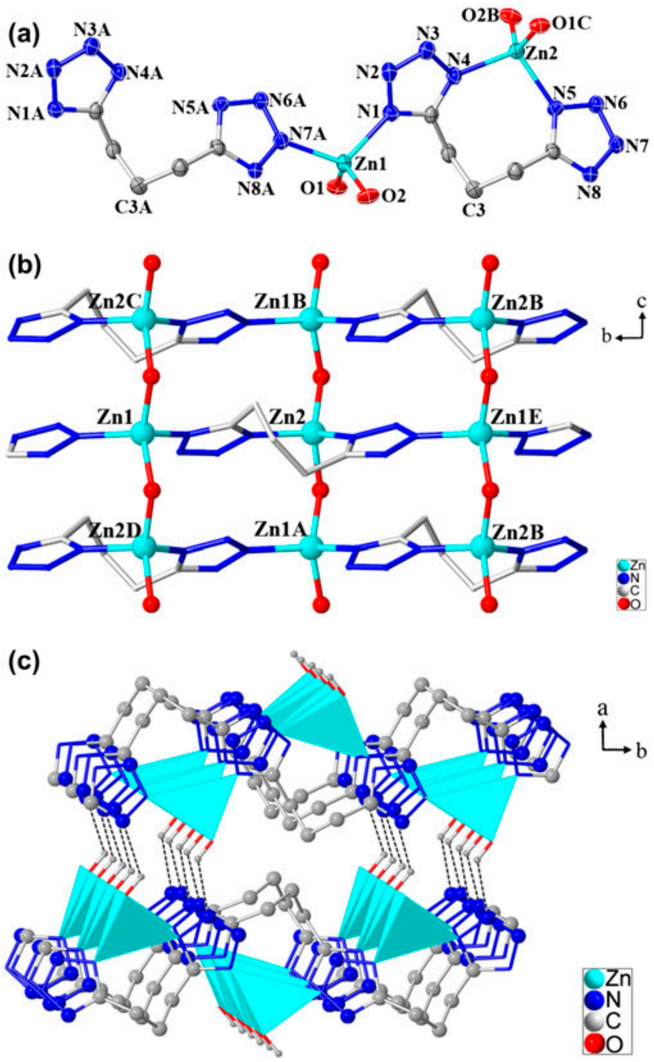

Figure 2. (a) Molecular structure of **2** with 50% thermal ellipsoid probabilities. Hydrogens are omitted for clarity. Symmetry codes: (A) $x, y + 1, z$, (B) $-x + 1/2, y - 1/2, z + 1/2$, (c) $-x + 1/2, y - 1/2, z - 1/2$; (b) view of 2-D layer in **2** along the *a* axis; (c) view of the 3-D supramolecular network in **2** formed through hydrogen bonds between the hydroxyl groups and the N atoms of the dtp^{2-} ligand.

two N atoms from two different dtp^{2-} anions, while Zn(2) is coordinated by two N atoms from different tetrazolate rings of the same dtp^{2-} anion, to form an eight-membered chelate. The Zn–N bond distances range from 2.023(3) to 2.060(3) Å, which are close to those in the equatorial plane of **1**, but they are longer than the Zn–O bond distances in **2** of 1.924(4) and 1.940(4) Å. Different from **1**, the two tetrazolate rings exhibit different bridging modes, one adopts a μ-1,3-bridging mode, while the other shows a μ-1,4-bridging mode (scheme 1). The same μ-1,4-bridging mode was also found in [Zn(dte)(H$_2$O)]$_n$ [20]. The twisting angle between the two tetrazolate rings in **2** is 40.358°, which is larger than that of the dte$^{2}-$ ligand in **1**. All bond distances and angles in the tetrazolate rings of the dtp^{2-} ligand are in the normal range and similar to those in **1**, hence the different coordination mode of the tetrazolate rings in **2** has no obvious effect on the metrical parameters. The dtp^{2-} anion links three Zn(II) cations via a chelating and bridging mode into a 1-D $[Zn_2(dtp)]_n$ chain [figure 2(b)]. The Zn···Zn distances bridged by the μ-1,3 and μ-1,4-tetrazolate rings are 6.028 and 6.127 Å, respectively. The hydroxyl groups alternatively bridge the Zn(1) and Zn(2) atoms to form a 1-D $[Zn_2(OH)_2]_n$ chain. The Zn···Zn distances bridged by O1 and O2 are 3.432 and 3.412 Å, respectively. The fusion of the $[Zn_2(dtp)]_n$ and $[Zn_2(OH)_2]_n$ chains results in the formation of 2-D layers [figure 2(b)]. The hydrogen bonds between the hydroxyl groups and dtp^{2-} N atoms [O1–H1···$N8^{i}$ 2.823(6), O1–H1···$N8^{i}$ 134.51°, O2–H2···$N3^{ii}$ 3.044(6) Å, O2–H2···$N3^{ii}$ 142.14, symmetry code: (i) $-x + 1, -y, z + 1/2$, (ii) $x + 1/2, -y + 1/2, z$] extend the 2-D layers into a 3-D supramolecular network [figure 2(c)].

3.3. *X-ray powder diffraction*

Powder X-ray diffraction shows that the experimental patterns are in good agreement with the theoretical ones generated from the single-crystal X-ray data [figure 3(a) and (b)], which clearly indicates the phase purity of **1** and **2**.

3.4. *Thermogravimetric analysis*

Both **1** and **2** are stable in air and their thermal stability was measured by thermogravimetric analysis (TGA) on polycrystalline samples under a nitrogen atmosphere (figure 4). A weight

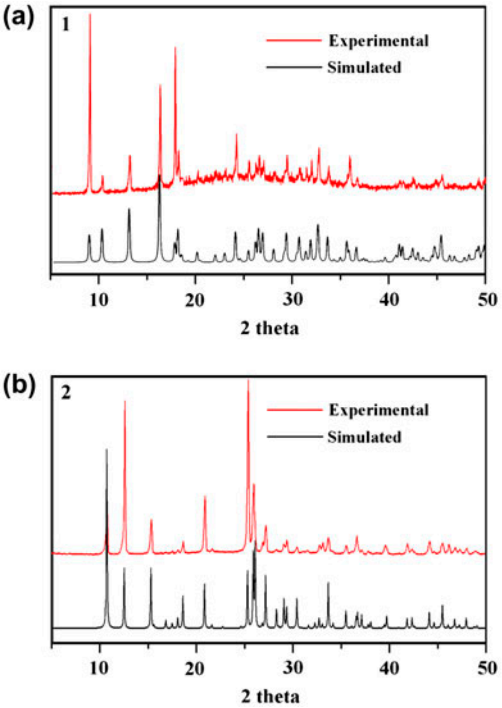

Figure 3. (a) Simulated and experimental powder X-ray diffraction patterns for **1**; (b) simulated and experimental powder X-ray diffraction patterns for **2**.

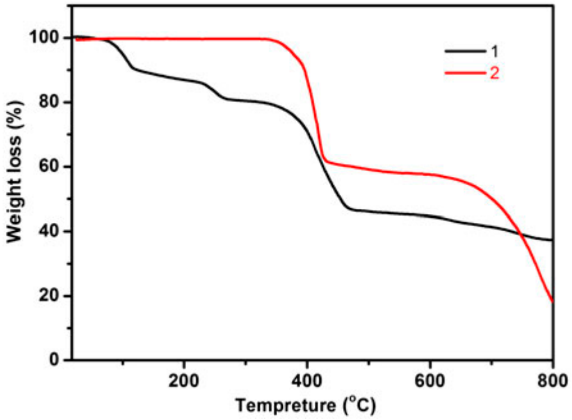

Figure 4. TGA curves of **1** and **2**.

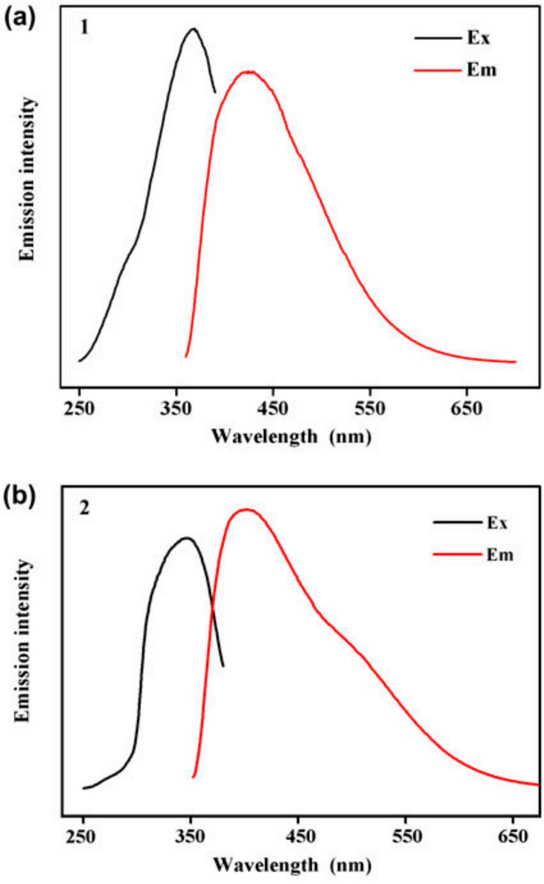

Figure 5. (a) Emission and excitation spectra of **1** at room temperature; (b) emission and excitation spectra of **2** at room temperature.

loss of 9.05 wt% before 115 °C for **1** can be attributed to the removal of lattice water and methanol molecules (Calcd: 9.02 wt%), and then CO_2 was liberated with the weight loss of 7.70 wt% (Calcd: 7.92 wt%) before 250 °C and subsequent collapse of the framework. The decomposition product at 470 °C corresponds to $Zn_2(CN)_3(N_3)$ (found: 46.53%, Calcd: 45.19%). The final product above 800 °C can be assigned as $Zn_2(CN)(N)$; the slightly higher residual weight at 800 °C (found: 37.35 wt%, Calcd: 30.77 wt%) can probably be ascribed to incomplete decomposition. Complex **2** starts to decompose above 340 °C and gave a material consistent with a 3:1 mixture of $Zn_2(CN)_4$ and ZnO as an intermediate at 428 °C (found: 62.39 wt%, Calcd: 60.89 wt%). Further heating to 800 °C did not give complete decomposition of this proposed intermediate. Obviously, the thermal stability of **2** is higher than that of **1**.

3.5. *Fluorescence property*

The solid-state fluorescence of **1** and **2** were investigated at room temperature, and their excitation and emission spectra are depicted in figure 5. The maximum emission peaks of **1** and **2** were observed at 403 ($\lambda_{ex} = 343$ nm) and 422 nm ($\lambda_{ex} = 367$ nm), respectively. In comparison with free H_2dte at 323 nm and H_2dtp at 480 nm [21], a blue shift for **1** and a red shift for **2** were observed. Thus, the luminescent emission may be ascribed to the coordination interaction between the flexible bis(tetrazolate) ligands and the Zn(II) center [21, 28–32].

4. Conclusion

Two zinc(II) coordination polymers with flexible bis(tetrazolyl) ligands have been synthesized. Owing to differences in flexibility and spacer length between the tetrazolate rings, the rings in the dte$^{2}-$ ligand in **1** adopt a $\mu_{1,4}$-bridging mode to join the Zn(II) ions, while the rings in the dtp^{2-} ligand in **2** connect the Zn(II) ions in both μ-1,3-bridging and μ-1,4-bridging modes. As a result, the dte^{2-} and dtp^{2-} anions link three Zn(II) ions in chelating and bridging coordination modes to form a 2-D layer and a 1-D chain, respectively. The 2-D layer in **1** and the 1-D chain in **2** further extend into 3-D and 2-D networks by anionic formate and hydroxyl bridges, respectively, which were formed *in situ*. This study demonstrated that flexible bis(tetrazolyl) ligands are promising for the construction of coordination polymers with unexpected structures.

Supplementary material

Crystallographic data for **1** and **2** have been deposited in the Cambridge Crystallographic Data Center as supplementary publication with CCDC numbers 951154 and 951155, respectively.

Funding

This work was supported by National Natural Science Foundation of China [grant number 21001025]; Natural Science Foundation of Fujian Province [grant number 2010J05017]; Provincial Education Department of Fujian [grant number JA12070].

References

[1] H. Gao, J.M. Shreeve. *Chem. Rev.*, **111**, 7377 (2011).
[2] R.H. Wang, H.Y. Xu, Y. Guo, R.J. Sa, J.M. Shreeve. *J. Am. Chem. Soc.*, **132**, 11904 (2010).
[3] X.X. Li, H.Y. Xu, F.Z. Kong, R.H. Wang. *Angew. Chem. Int. Ed.*, **52**, 13769 (2013).
[4] G. Steinhauser, T.M. Klapötke. *Angew. Chem. Int. Ed.*, **47**, 3330 (2008).
[5] G.W. Yang, B.J. Wang, Z.T. Shen, Q.Y. Li, C. Ji, X.F. Shen, M.H. He. *J. Coord. Chem.*, **65**, 2657 (2012).
[6] G.H. Tao, D.A. Parrish, J.M. Shreeve. *Inorg. Chem.*, **51**, 5305 (2012).
[7] M.H.V. Huynh, M.D. Coburn, T.J. Meyer, M. Wetzler. *Proc. Natl. Acad. Sci.*, **103**, 10322 (2006).
[8] S.W. Wang, L. Yang, T.L. Zhang, G.T. Zhang, J.G. Zhang, Z.N. Zhou. *J. Coord. Chem.*, **64**, 2583 (2011).
[9] P. Cui, Y.G. Ma, H.H. Li, B. Zhao, J.R. Li, P. Cheng, P.B. Balbuena, H.C. Zhou. *J. Am. Chem. Soc.*, **134**, 18892 (2012).
[10] P. Cui, L.J. Ren, Z. Chen, H.C. Hu, B. Zhao, W. Shi, P. Cheng. *Inorg. Chem.*, **51**, 2303 (2012).
[11] P. Cui, Z. Chen, D.L. Gao, B. Zhao, W. Shi, P. Cheng. *Cryst. Growth Des.*, **10**, 4370 (2010).
[12] L. Carlucci, G. Ciani, D.M. Proserpio. *Angew. Chem. Int. Ed.*, **38**, 3488 (1999).
[13] J. Wang, J.H. Nie, C.T. Dai. *J. Coord. Chem.*, **64**, 1645 (2011).
[14] Y. Tao, J.R. Li, Q. Yu, W.C. Song, X.L. Tong, X.H. Bu. *CrystEngComm*, **10**, 699 (2008).
[15] T.P. Hu, W.H. Bi, X.Q. Hu, X.L. Zhao, D.F. Sun. *Cryst. Growth Des.*, **10**, 3324 (2010).
[16] W.B. Chen, Y.X. Qiu, X.M. Lin, M. Yang, H. Yan, F.X. Gao, Z.J. Yang, W Dong. *J. Coord. Chem.*, **66**, 1700 (2013).
[17] G.H. Xu, T. Hang, K.J. Pan, Q. Ye. *J. Coord. Chem.*, **62**, 2457 (2009).
[18] M. Dincă, A.F. Yu, J.R. Long. *J. Am. Chem. Soc.*, **128**, 8904 (2006).
[19] A. Białońska, R. Bronisz, M.F. Rudolf, M. Weselski. *Inorg. Chem.*, **51**, 237 (2012).
[20] L. Shen, J. Yang, G.W. Yang, Q.Y. Li, X.Y. Tang, F. Zhou, Z.F. Miao, J.N. Jin, W. Shen. *Inorg. Chim. Acta*, **370**, 150 (2011).
[21] X.L. Tong, D.Z. Wang, T.L. Hu, W.C. Song, Y. Tao, XH Bu. *Cryst. Growth Des.*, **9**, 2280 (2009).
[22] X.J. Li, X.F. Guo, X.L. Weng, S. Lin. *CrystEngComm*, **14**, 1412 (2012).
[23] X.J. Li, X.L. Weng, R.J. Tang, Y.M. Lin, Z.L. Ke, W.B. Zhou, R. Cao. *Cryst. Growth Des.*, **10**, 3228 (2010).
[24] X.F. Guo, X.J. Li, X.L. Weng, S. Lin. *J. Mol. Struct.*, **1008**, 63 (2012).
[25] X.J. Li, G.C. Ma, X.H. Xu. *J. Coord. Chem.*, **66**, 3249 (2013).
[26] V.Y. Zubarev, R.E. Trifonov, V.V. Poborchii, V.A. Ostrovskii. *Chem. Heterocycl. Compd.*, **42**, 469 (2006).
[27] G.M. Sheldrick. *SHELXL97, Program for Crystal Structure Refinement*, University of Göttingen, Göttingen, Germany (1997).
[28] L.Z. Chen, J. Zou, Y.M. Gao, S. Wan, M.N. Huang. *J. Coord. Chem.*, **64**, 715 (2011).
[29] X.W. Wang, J.Z. Chen, J.H. Liu. *Cryst. Growth Des.*, **7**, 1227 (2007).
[30] G.J. Xu, Y.H. Zhao, K.Z. Shao, Y.Q. Lan, X.L. Wang, Z.M. Su, L.K. Yan. *CrystEngComm*, **11**, 1842 (2009).
[31] B.T. Liu, D. Zhao, T. Li, X.R. Meng. *J. Coord. Chem.*, **66**, 139 (2013).
[32] G.X. Liu, Y.Q. Huang, Q. Chu, T. Okamura, W.Y. Sun, H. Liang, N. Ueyama. *Cryst. Growth Des.*, **8**, 3233 (2008).